2011 American Control Conference
on O'Farrell Street, San Francisco, CA, USA
June 29 - July 01, 2011

Robust Estimation of the Friction Forces Generated by Each Tire of a Vehicle

Tesheng Hsiao, *Member, IEEE*, Nien-Chi Liu, and Syuan-Yi Chen

Abstract—**Real-time information of tire friction forces is invaluable for vehicle control systems, such as ABS and the electronic stability program (ESP), to achieve better stability and maneuverability. To estimate tire forces on-line, this paper proposes a robust tire force estimation algorithm which is able to identify the longitudinal and lateral tire forces of each individual wheel. In addition, the estimation results are robust w.r.t variations in vehicle parameters. The dependency between the longitudinal and lateral tire forces is explicitly taken into account by incorporating friction ellipses into the estimation algorithm. Simulations based on a 14-degree-of-freedom nonlinear vehicle model are conducted and the results are satisfactory, even in the presence of sudden changes of the road conditions and variations in vehicle parameters.**

I. Introduction

The interaction between the tire and the road is the primary mechanism that converts engine/steering torques to traction/cornering forces of ground vehicles; therefore real- time information of the tire friction forces is invaluable to the vehicle control systems since increasingly stringent requirements of safety and maneuverability are imposed on modern automobiles.

Estimation of tire friction forces becomes an active research topic recently [1]. A variety of estimation techniques have been proposed in the literature. Most of them are based on either tire models or vehicle models. The simplest longitudinal tire model assumes that the longitudinal tire force is linearly proportional to the tire slip ratio, which is the relative difference between the translational velocity and the angular velocity of a wheel. Depending on the way to obtain the vehicle's velocity and to estimate the "slip-slop", i.e. the proportional constant between the longitudinal tire force and the slip ratio, various slip-based methods were proposed. For example, Gustafsson [2] used the undriven wheel's speed as the reference velocity of the vehicle; however application is restricted to the cases of front- (or rear-) wheel drive vehicles in acceleration. Wang *et al.* used the differential global positioning systems (DGPS) to obtain more accurate estimate of the vehicle's velocity and extend the slip-slop method to all-wheel drive vehicles for both accelerating and braking cases [3].

Tesheng Hsiao is with the Department of Electrical Engineering, National Chiao Tung University, Hsinchu, Taiwan (TEL: 886-3-5131249; FAX: 886-3- 5715998; e-mail: tshsiao@cn.nctu.edu.tw).

Nien-Chi Liu is with the Department of Electrical Engineering, National Chiao Tung University, Hsinchu, Taiwan (e-mail: ncliu.ece97g@nctu.edu.tw).

Syuan-Yi Chen is with the Information and Communications Research Laboratories (ICL), Industrial Technology Research Institute (ITRI), Hsinchu, Taiwan (email: chensy@itri.org.tw).

The linear slip-slop model is valid only in the low slip ratio region. To estimate the longitudinal tire force in high slip ratio conditions, nonlinear tire models must be considered. Burckhardt model and LuGre model were explored in [4] and [5] respectively along with steepest descent adaptive algorithms to identify the parameters of the tire models as well as the road friction coefficient. On the other hand, nonlinear tire models were also used in the estimation of lateral tire forces [6].

The inherent limitations of the tire-model-based approaches are the validity of the tire models in use. Note that a lot of tire models have been proposed in the literature, including various analytical/experimental and static/dynamic tire models [1]. These models differ in their degrees of accuracy and complexity; however none of them can completely describe all aspects of the tire behavior while keeps the model as simple as possible. Thus it is crucial to fully comprehend the restrictions imposed by a particular tire model before the associated tire-model-based approach is applied. Besides, many tire models are developed for the tire force in either the longitudinal or the lateral direction; however it is well-known that the tire forces in both directions are dependent. Generally speaking, the more the longitudinal tire force is established for traction/braking, the less the lateral tire force is available for cornering, and vice versa. Therefore a longitudinal (lateral) tire force estimation algorithm without considering the effects of the other direction may perform poorly when the vehicle is in a combined motion of traction/braking and cornering.

To simultaneously estimate the longitudinal and lateral tire forces, the vehicle dynamics were exploited. Ray [7] set up an 8-degree-of-freedom nonlinear vehicle model and treated tire forces in both directions of each wheel as additional state variables. Then all state variables were estimated by the extended Kalman filter (EKF). Furthermore, Bayesian hypotheses were used to classify the road condition based on the estimated tire forces. Note that no particular tire model was assumed in Ray's method. In [8], the longitudinal tire force of each wheel was estimated using the moment balance equation of each wheel; then estimates of lateral tire forces were found through a simplified vehicle model; however, only the sums of the front and rear lateral tire forces can be identified. Baffet, Charara, and Lechner [9] proposed a sliding mode observer to estimate the longitudinal and lateral tire forces simultaneously based on a simplified vehicle model; however the rear tires were assumed in pure rolling and hence their longitudinal tire forces were neglected. Besides, only the sums of the front and rear lateral tire forces can be obtained.

Although the integrated estimation of the longitudinal and lateral tire forces has been addressed recently, identifying lateral tire forces of each individual wheel is still an open question. Moreover, vehicle-model-based methods are susceptible to model uncertainties. The contribution of this paper is that we propose a tire force estimation algorithm which is able to identify tire forces in *both directions* of *each individual wheel* and is *robust* w.r.t variations in vehicle parameters. The proposed algorithm consists of three consecutive steps: longitudinal tire force estimation, lateral tire force estimation, and vehicle parameter estimation. The estimation of the longitudinal tire force is based on the moment balance equation of each wheel. Then lateral tire forces are solved by using a simplified vehicle model and the *friction ellipses* which accounts for the dependency between the longitudinal and lateral tire forces. Finally, a maximum likelihood parameter estimator is implemented to estimate the critical vehicle parameters on-line such that the effects of parameter uncertainties on the tire force estimates are alleviated. Then we verify the performance of the proposed algorithm by simulations under various road conditions and parameter variations.

This paper is organized as follows. Section II introduces the fundamental notions of tire models. The proposed algorithm is presented in Section III and simulation results are discussed in Section IV. Section V concludes this paper.

I. Notions of Tire Forces

Figure 1 illustrates the tire force decomposed in the longitudinal direction (F_a) and in the lateral direction (F_b). v_w is the wheel's velocity and δ is the steering angle.

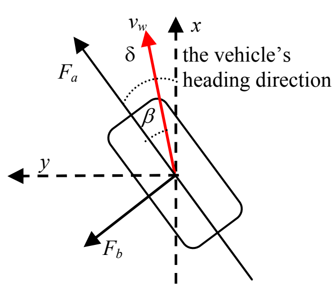

Figure 1: Decomposition of the tire force into the longitudinal and lateral directions. β and δ are the tire slip angle and steering angle respectively..

The longitudinal tire force is a function of the tire slip ratio, the normal tire force, and the road friction coefficient. The tire slip ratio is defined as follows:

$$\sigma = \frac{R_e\omega - v_w\cos\beta}{\max\left\{R_e\omega, v_w\cos\beta\right\}} \qquad (1)$$

where R_e is the effective tire radius and ω is the angular velocity of the tire. β is called the tire slip angle, which is the angle between the tire's heading direction and the direction of the tire velocity v_w. See Figure 1.

On the other hand, the lateral tire force is a function of the tire slip angle, the normal tire force, and the road friction coefficient. One of the commonly used tire models is the following "magic formula" [10]:

$$F_i(\lambda) = \mu D_i \sin\left\{C_i \tan^{-1}\left[B_i\lambda - E_i\left(B_i\lambda - \tan^{-1}\left(B_i\lambda\right)\right)\right]\right\} \quad (2)$$

where F_i, i=a,b, is either the longitudinal or the lateral tire force. The independent variable λ denotes the slip ratio for the longitudinal tire force, or the slip angle for the lateral tire force. μ is the road friction coefficient. B_i, C_i, D_i, and E_i are parameters of the magic formula whose values vary with the normal tire force.

The graph of (2) is shown in Figure 2 for various normal tire forces and road friction coefficients. The upper (lower) rows of Figure 2 are the longitudinal (lateral) tire forces v.s. the slip ratio (slip angle) for different normal tire forces (left column) and road friction coefficients (right column). It can be seen that for a fixed road friction coefficient, if the slip ratio (slip angle) is small, the longitudinal (lateral) tire force is proportional to the slip ratio (slip angle), irrespective of the normal tire forces.

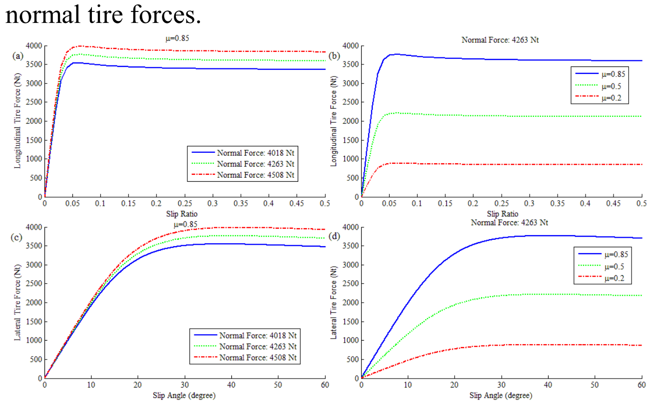

Figure 2: (a) Longitudinal tire forces v.s. slip ratios for various normal tire forces when μ=0.85, and (b) various road friction coefficients when the normal tire force is 4263 Nt. (c) Lateral tire forces v.s. slip angles for various normal tire forces when μ=0.85, and (d) various road friction coefficients when the normal tire force is 4263 Nt.

II. Tire Force Estimation

The proposed tire force estimation algorithm consists of three steps in order: longitudinal tire force estimation, lateral tire force estimation, and parameter estimation. The block diagram is illustrated in Figure 3.

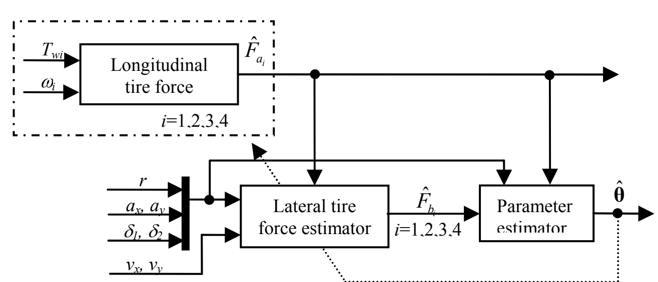

Figure 3: The block diagram of the proposed robust tire force estimation algorithm

The inputs to the longitudinal tire force estimator include the torques applied to each wheel and the angular velocities of each wheel. These inputs are measurable by torque sensors and speed sensors respectively. To estimate the lateral tire forces, the proposed algorithm requires the vehicle's yaw rate, steering angles of the two front wheels, longitudinal and lateral accelerations and velocities of the vehicle's center of gravity (C.G.). The yaw rate and the accelerations are available through the on-board inertia navigation system. The velocity of the vehicle's C.G. can be obtained if on-board DGPS is available [6]. These measured data along with the estimated tire forces are sent to the parameter estimator which updates the critical parameters used in the lateral tire force estimator in order to compensate for parameter variations.

A. Longitudinal Tire Force Estimation

The moment balance equation of each wheel is used to estimate the longitudinal tire force. The same approach was adopted in [8] too. Consider a tire rolling on a surface as shown in Figure 4. Then

$$I_w \dot{\omega} = T_w - R_e F_a \tag{3}$$

where I_w, ω, R_e are the moment of inertia, angular velocity, and effective radius of the wheel respectively. T_w denotes the torque applied to the wheel due to braking or traction.

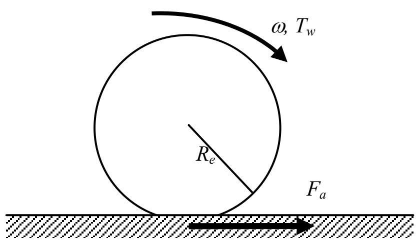

Figure 4: Longitudinal Tire Force

Suppose that T_w and ω are measurable. The angular acceleration can be approximated by the backward difference of ω when the proposed algorithm is implemented in the discrete-time domain:

$$\hat{\dot{\omega}}(k) = \frac{\omega(k) - \omega(k-1)}{T_s} \tag{4}$$

where the index k denotes the k^{th} time step and T_s is the sampling time. Assume that the deformation of the tire is negligible, i.e. $R_e \approx R$, where R is the undeformed tire radius. Then the longitudinal tire force is estimated by

$$\hat{F}_a = \frac{T_w - I_w \hat{\dot{\omega}}}{R} \tag{5}$$

Note that (5) depends on I_w and R which are properties of the tire and are assumed to be known exactly. Therefore (5) is immune to the variations in vehicle's parameters introduced in subsequent subsections.

B. Lateral Tire Force Estimation

The longitudinal and lateral tire forces of all wheels of a vehicle are illustrated in Figure 5. For easy reference, the four wheels are labeled as 1, 2, 3, and 4, representing the front left, front right, rear right, and rear left wheels respectively. δ_1 and δ_2, the steering angles of the front left and front right wheels respectively, satisfy the Ackerman steering geometry when the vehicle is negotiating a turn [11]: $\cot\delta_o - \cot\delta_i = \frac{b_f}{l}$, where δ_i and δ_o denote the steering angles of the inner front wheel and the outer front wheel respectively. l and b_f are the wheelbase and the front track width respectively.

Let F_{xi} and F_{yi}, i=1,2,3,4, denote the tire forces decomposed along the x and y axes of the vehicle's body frame. Then

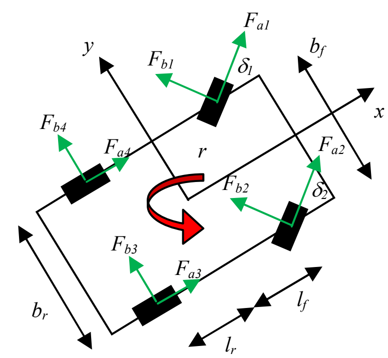

Figure 5: Longitudinal and lateral tire forces of a vehicle

$F_{xi}=F_{ai}\cos\delta_i - F_{bi}\sin\delta_i$, $\quad F_{yi}=F_{ai}\sin\delta_i + F_{bi}\cos\delta_i$, $\quad i$=1,2 (6)

$F_{xj}=F_{aj}$, $\quad F_{yj}=F_{bj}$, $\quad j$=3,4 (7)

The Newton's 2nd law leads to

$$ma_x = \sum_{i=1}^{4} F_{x_i}, \; ma_y = \sum_{i=1}^{4} F_{y_i}, \; I_z \dot{r} = M_z \tag{8}$$

where m, I_z and M_z are the mass, the moment of inertia and the external moment around the z axis of the vehicle. a_x and a_y, are the accelerations of the vehicle's C.G. along the x and y directions respectively. r is the yaw rate. It is obvious that

$$M_z = \left(F_{x_2} - F_{x_1}\right)\frac{b_f}{2} + \left(F_{x_3} - F_{x_4}\right)\frac{b_r}{2} + \left(F_{y_1} + F_{y_2}\right)l_f - \left(F_{y_3} + F_{y_4}\right)l_r$$

l_f and l_r are the distances from the vehicle's C.G. to the front and rear axles respectively. b_f and b_r are the front and rear track widths respectively. See Figure 5. Suppose that the yaw rate is measurable. The first directive of the yaw rate can be approximated the backward difference of r:

$$\hat{\dot{r}}(k) = \frac{r(k) - r(k-1)}{T_s} \tag{9}$$

Rearrange (6), (7), (8), and (9) in a matrix form and replace the longitudinal tire forces with their estimates in (5). Then

$$\mathbf{A}\mathbf{F}_b = \mathbf{b} \tag{10}$$

where $\mathbf{F}_b=[F_{b1}, F_{b2}, F_{b3}+F_{b4}]^T$,

$$\mathbf{A} = \begin{bmatrix} -\sin\delta_1 & -\sin\delta_2 & 0 \\ \cos\delta_1 & \cos\delta_2 & 1 \\ l_f\cos\delta_1 + \frac{b_f}{2}\sin\delta_1 & l_f\cos\delta_2 - \frac{b_r}{2}\sin\delta_2 & -l_r \end{bmatrix},$$

$$\mathbf{b} = \begin{bmatrix} ma_x - \hat{F}_{a_1}\cos\delta_1 - \hat{F}_{a_2}\cos\delta_2 - \hat{F}_{a_3} - \hat{F}_{a_4} \\ ma_y - \hat{F}_{a_1}\sin\delta_1 - \hat{F}_{a_2}\sin\delta_2 \\ b_3 \end{bmatrix}$$

$$b_3 = I_z \hat{r} + \left(\hat{F}_{a_1} \sin\delta_1 + \hat{F}_{a_2} \sin\delta_2\right) l_f$$
$$-\left(\hat{F}_{a_2} \cos\delta_2 - \hat{F}_{a_1} \cos\delta_1\right) \tfrac{b_f}{2} - \left(\hat{F}_{a_3} - \hat{F}_{a_4}\right) \tfrac{b_r}{2}$$

If δ_1 and δ_2 are sufficiently large, then **A** is nonsingular. Thus we can define $\hat{\mathbf{F}}_b^d = \mathbf{A}^{-1}\mathbf{b}$. On the other hand, if $\delta_1 \approx \delta_2 << 1$, then **A** is nearly singular. In such a case, (10) degenerates to

$$\begin{bmatrix} 1 & 1 \\ l_f & -l_r \end{bmatrix} \begin{bmatrix} F_{b_f} \\ F_{b_r} \end{bmatrix} = \begin{bmatrix} ma_y \\ I_z \hat{r} \end{bmatrix}$$

where $F_{bf}=F_{b1}+F_{b2}$ and $F_{br}=F_{b3}+F_{b4}$. Hence the estimates of the front and rear lateral tire forces for a small steering angle are

$$\begin{bmatrix} \hat{F}_{b_f} \\ \hat{F}_{b_r} \end{bmatrix} = \begin{bmatrix} 1 & 1 \\ l_f & -l_r \end{bmatrix}^{-1} \begin{bmatrix} ma_y \\ I_z \hat{r} \end{bmatrix}$$

If the steering angle is small, the difference between F_{b1} and F_{b2} is negligible; therefore we define $\hat{\mathbf{F}}_b^s = \left[\frac{\hat{F}_{bf}}{2}, \frac{\hat{F}_{bf}}{2}, \hat{F}_{br}\right]^T$. Note that both $\hat{\mathbf{F}}_b^d$ and $\hat{\mathbf{F}}_b^s$ are estimates of $\mathbf{F}_b$. The former is preferred in the case of large steering angles because F_{b1} and F_{b2} can be identified distinctly while the latter is applied in the case of small steering angles. To avoid discontinuity in the estimated $\mathbf{F}_b$ due to the switching between $\hat{\mathbf{F}}_b^s$ and $\hat{\mathbf{F}}_b^d$ as the steering angle changes, the following lateral tire force estimate is proposed:

$$\hat{\mathbf{F}}_b = g_d \hat{\mathbf{F}}_b^d + g_s \hat{\mathbf{F}}_b^s \qquad (11)$$

where $g_d \propto \frac{1}{\kappa(\delta_1,\delta_2)}$, $g_s \propto \frac{1}{\kappa_0}$, and $g_1+g_2=1$. $\kappa(\delta_1,\delta_2)$ is the condition number of **A**, which is a function of δ_1 and δ_2. κ_0 is a fixed number which is chosen in a way that the computation of $\mathbf{A}^{-1}$ suffers from no numerical problems as long as $\kappa(\delta_1,\delta_2)<\kappa_0$.

Note that the lateral tire forces of the two front wheels can be identified from (11); however only the sum of the two rear lateral tire forces is available. This is because solving F_{bi}, i=1,2,3,.4 from the set of equations (8) is an underconstrained problem. To add more constraints, we introduce the friction ellipse in the next subsection.

C. Friction Ellipses

If a tire establishes longitudinal and lateral tire forces simultaneously, then the tire forces in both directions satisfy the following friction ellipse constraints [12]:

$$\left(\frac{F_{a_i}}{\overline{F}_{a_i}}\right)^2 + \left(\frac{F_{b_i}}{\overline{F}_{b_i}}\right)^2 = 1, \quad i=1,2,3,4 \qquad (12)$$

F_{a_i} and F_{b_i} are the longitudinal and lateral tire forces respectively when the vehicle is in a combined motion of traction/braking and concerning. Given the same normal tire forces, road friction coefficient, slip ratio and slip angle, $\overline{F}_{a_i}$ is the longitudinal tire force of the i^{th} wheel if the vehicle is *not* negotiating a turn, and $\overline{F}_{b_i}$ is the lateral tire force of the i^{th} wheel if the vehicle is *not* accelerating or decelerating. Note that $F_{a_i} \le \overline{F}_{a_i}$ and $F_{b_i} \le \overline{F}_{b_i}$.

(12) imposes explicit constraints on F_{a_i} and F_{b_i}; however more unknown variables $\overline{F}_{a_i}$ and $\overline{F}_{b_i}$ are introduced at the same time, leaving a set of underconstrained equations (8) and (12). To make the problem solvable, we assume that the slip ratios and slip angles of all wheels are small, and the road friction coefficients of all wheels are identical. Under these circumstances, we have observed in Figure 2 that the longitudinal (lateral) tire force is proportional to the slip ratio (slip angle) and is independent of the normal tire force. Therefore there exist constants K_a and K_b such that

$$\overline{F}_{a_i} = K_a \sigma_i, \quad \overline{F}_{b_i} = K_b \beta_i, \quad i=1,2,3,4 \qquad (13)$$

σ_i i=1,2,3,4, is the slip ratio defined in (1). The speed of the i^{th} wheel is

$$\left|v_{w_1}\right| = \sqrt{\left(v_x - \tfrac{b_f}{2} r\right)^2 + \left(v_y + l_f r\right)^2}, \quad \left|v_{w_2}\right| = \sqrt{\left(v_x + \tfrac{b_f}{2} r\right)^2 + \left(v_y + l_f r\right)^2}$$
$$\left|v_{w_3}\right| = \sqrt{\left(v_x + \tfrac{b_r}{2} r\right)^2 + \left(v_y - l_r r\right)^2}, \quad \left|v_{w_4}\right| = \sqrt{\left(v_x - \tfrac{b_r}{2} r\right)^2 + \left(v_y - l_r r\right)^2}$$

β_i, i=1,2,3,4, is the slip angle of the i^{th} wheel and can be calculated as follows:

$$\beta_1 = \delta_1 - \tan^{-1}\left(\frac{v_y + l_f r}{v_x - \frac{1}{2} b_f r}\right), \quad \beta_2 = \delta_2 - \tan^{-1}\left(\frac{v_y + l_f r}{v_x + \frac{1}{2} b_f r}\right)$$
$$\beta_3 = -\tan^{-1}\left(\frac{v_y - l_r r}{v_x + \frac{1}{2} b_r r}\right), \quad \beta_4 = -\tan^{-1}\left(\frac{v_y - l_r r}{v_x - \frac{1}{2} b_r r}\right)$$

If we define

$$t_{ij} = \frac{\sigma_i}{\sigma_j} \text{ and } n_{ij} = \frac{\beta_i}{\beta_j}, \ i,j=1,2,3,4, \qquad (14)$$

then from (13) we have

$$\overline{F}_{a_i} = t_{ij} \overline{F}_{a_j} \text{ and } \overline{F}_{b_i} = n_{ij} \overline{F}_{b_j}, \ i,j=1,2,3,4. \qquad (15)$$

Direct computation based on (12), (14), and (15) yields

$$F_{b_3} = \pm \frac{\sqrt{1 - \left(\frac{t_{43} F_{a_3}}{\overline{F}_{a_4}}\right)^2}}{\sqrt{1 - \left(\frac{F_{a_4}}{\overline{F}_{a_4}}\right)^2}} n_{34} F_{b_4} \qquad (16)$$

Note that t_{ij} and n_{ij} can be calculated from measured data. Also recall that

$$F_{b_3} + F_{b_4} = F_{b_r} \qquad (17)$$

Substitute estimated F_{ai} and F_{br} into (16) and (17); then we can solve these two equations simultaneously to find out the estimates of the lateral tire forces of the rear wheels.

D. Parameter Estimation

The estimation of the lateral tire forces depends on the vehicle model whose parameters are uncertain. From (10) we recognize that uncertain parameters m, I_z, l_f and l_r, or equivalently the position of the vehicle's C.G., are involved in the estimation of lateral tire forces. In order to enhance the robustness of the tire force estimation, we implement a maximum likelihood parameter estimator to update these critical parameters on-line.

Let $\boldsymbol{\theta}$ be the vector of the vehicle parameters, i.e.

$$\boldsymbol{\theta} = \begin{bmatrix} m & I_z & s \end{bmatrix}^T \quad (18)$$

where s denotes the displacement of the vehicle's C.G. from its nominal position towards the front of the vehicle. Therefore the external moment applied to the vehicle with the C.G. shifted by an amount of s is

$$M_z = \left(F_{x_2} - F_{x_1}\right)\frac{b_f}{2} + \left(F_{x_3} - F_{x_4}\right)\frac{b_r}{2} + \left(F_{y_1} + F_{y_2}\right)\left(l_f - s\right) - \left(F_{y_3} + F_{y_4}\right)\left(l_r + s\right)$$

Consequently, (8) can be rewritten as $\mathbf{P}\boldsymbol{\theta}=\mathbf{u}$, where

$$\mathbf{P} = \begin{bmatrix} a_x & 0 & 0 \\ a_y & 0 & 0 \\ 0 & \dot{r} & \sum_{i=1}^{4} F_{y_i} \end{bmatrix}, \quad \mathbf{u} = \begin{bmatrix} \sum_{i=1}^{4} F_{x_i} \\ \sum_{i=1}^{4} F_{y_i} \\ M_z|_{s=0} \end{bmatrix}$$

The value of $\mathbf{u}$ has been estimated in previous subsections. Now consider the following discrete-time "fictitious system":

$$\mathbf{x}(k+1) = \alpha\mathbf{x}(k) + (1-\alpha)\mathbf{u}(k) + \mathbf{w}(k)$$
$$\mathbf{y}(k) = \mathbf{x}(k) + \mathbf{v}(k)$$

where $0<\alpha<1$, so the system is stable. $\mathbf{w}(k)$ and $\mathbf{v}(k)$ are the process noise and measurement noise respectively. They are assumed to be Gaussian distributed with zero means and covariance matrices $\mathbf{Q}$ and $\mathbf{R}_v$ respectively. $\mathbf{x}(k)$ is the state of the fictitious system and is evaluated by filtering each element of $\mathbf{u}(k)$ through the discrete-time filter $\frac{(1-\alpha)z^{-1}}{1-\alpha z^{-1}}$.

Note that $\mathbf{u}(k)=\mathbf{P}(k)\boldsymbol{\theta}$, and we would like to find an estimate of $\boldsymbol{\theta}$ with maximum likelihood. Let $p(\cdot)$ denote the probability density function and $\mathbf{x}(1{:}k)$ denote the set $\{\mathbf{x}(1),\ldots,\mathbf{x}(k)\}$. Then the likelihood function up to time step k is:

$$p\left(\mathbf{x}(0:k)\,|\,\boldsymbol{\theta}\right) = p\left(\mathbf{x}(0)\,|\,\boldsymbol{\theta}\right)\prod_{i=1}^{k} p\left(\mathbf{x}(i)\,|\,\mathbf{x}(i-1),\boldsymbol{\theta}\right)$$

where $p\left(\mathbf{x}(0)\,|\,\boldsymbol{\theta}\right) \propto \exp\left\{\frac{-1}{2}\mathbf{x}^T(0)\mathbf{Q}^{-1}\mathbf{x}(0)\right\}$ and

$$p\left(\mathbf{x}(i)\,|\,\mathbf{x}(i-1),\boldsymbol{\theta}\right) \propto \exp\left\{-\frac{1}{2}\left(\mathbf{x}(i)-\alpha\mathbf{x}(i-1)-(1-\alpha)\mathbf{u}(i-1)\right)^T \cdot \mathbf{Q}^{-1}\left(\mathbf{x}(i)-\alpha\mathbf{x}(i-1)-(1-\alpha)\mathbf{u}(i-1)\right)\right\}$$

Take the first derivative of the logarithm of $p\left(\mathbf{x}(0:k)\,|\,\boldsymbol{\theta}\right)$ w.r.t. $\boldsymbol{\theta}$ and set the result to zero. Then we have

$$\frac{\partial}{\partial\boldsymbol{\theta}}\log p\left(\mathbf{x}(0:k)\,|\,\boldsymbol{\theta}\right) \propto \sum_{i=1}^{k}\mathbf{P}^T(i-1)\mathbf{Q}^{-1}\left(\mathbf{x}(i)-\alpha\mathbf{x}(i-1)-(1-\alpha)\mathbf{P}(i-1)\boldsymbol{\theta}\right) = 0$$

Therefore the maximum likelihood estimate of $\boldsymbol{\theta}$ is:

$$\hat{\boldsymbol{\theta}} = \frac{1}{1-\alpha}\left[\left(\sum_{i=1}^{k}\mathbf{P}^T(i-1)\mathbf{Q}^{-1}\mathbf{P}(i-1)\right)\right]^{-1} \cdot \left[\sum_{i=1}^{k}\mathbf{P}^T(i-1)\mathbf{Q}^{-1}\left(\mathbf{x}(i)-\alpha\mathbf{x}(i-1)\right)\right]$$

According to the estimated $\boldsymbol{\theta}$, we update the corresponding parameters in (10). Therefore the lateral tire force estimation at the next time step is based on the up-to-date vehicle parameters, so the estimation result is robust w.r.t parameter variations.

III. SIMULATION

In this section, we evaluate the performance and robustness of the proposed tire force estimation algorithm by simulations. First of all, a 14-degree-of-freedom (DOF) nonlinear vehicle model [13] and the magic formula are established to simulate the vehicle's dynamics and tire forces. This nonlinear vehicle model includes the 6-DOF motion of the sprung mass of the vehicle, and the rolling and suspension displacements of the 4 wheels. The following parameters are used in the nonlinear vehicle model:

m=1740Kg, I_z=2961Kg·m^2, l_f=0.9m, l_r=1.55m, b_f=1.65m, b_r=1.45m

Gaussian noise is added to a_x, a_y, r, and ω_i, i=1,2,3,4, to simulate measurement noise. The Gaussian noise is assumed to have zero mean and unit variance.

Because the backward difference in (4) and (9) tends to amplify high frequency noise, all sensor measurements are filtered through 2nd order lowpass Butterworth filters with cutoff frequency at 20 Hz before the sensor data are applied to tire force estimators. The proposed algorithm is implemented in the discrete-time domain with sampling time 1ms.

Now we consider the case that the vehicle is simultaneously braking and turning left. At the same time, the road condition changes. The braking torque applied to each wheel is 100 Nt. The steering angle is 0 before t=7sec, and increases to 0.1 rad at the next second. The road friction coefficient μ is 0.85 for t=0~8 sec, 0.65 for t=8~14 sec, and 0.45 for t=14~20 sec. The steering angle of the front right wheel and the road friction coefficient are shown in Figure 6.

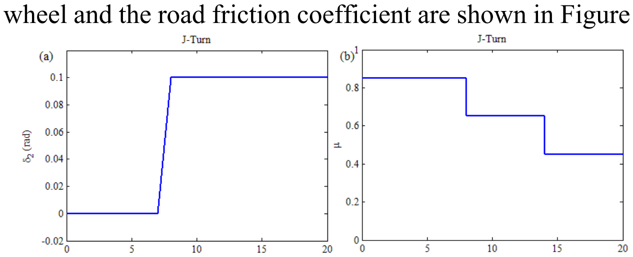

Figure 6: (a) the steering angle of the front right wheel. (b) the road friction coefficient

For lateral tire force estimation, three cases are considered:

- case (i): $\boldsymbol{\theta}$ (see (18)) is known exactly.
- case (ii): $\boldsymbol{\theta}$ differs from its nominal value, but the parameter estimator is turned off.
- case (iii): $\boldsymbol{\theta}$ differs from its nominal value, and the parameter estimator is turned on.

In case (ii) and (iii), we assume that the parameters used in the lateral tire force estimator are

m=1940Kg, I_z=3480 Kg·m^2, l_f=1.05m, l_r=1.4m.

Note that if we choose s=0 for this pair of l_f and l_r, then the true l_f and l_r corresponds to s=0.15m.

The proposed algorithm starts at t=5 sec at which the vehicle's transient response due to its initial conditions has vanished. Figure 7 demonstrates that the estimated longitudinal tire forces of all wheels closely follow the real tire forces, in spite of sudden changes of the road friction coefficient.

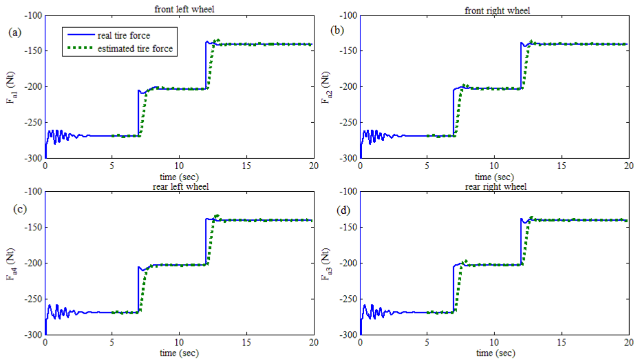

Figure 7: Real (solid line) and estimated (dotted line) longitudinal tire forces for the front left (a), front right (b), rear left (c) and rear right (d) wheels.

On the other hand, the estimated lateral tire forces are shown in Figure 8. Figure 8(a)(b)(d)(e) illustrate the results of case (i) and (iii), while the results of case (ii) are shown in Figure 8(c)(d). This separated demonstration is due to the huge difference in the scales of the estimated tire forces between case (ii) and the others. From Figure 8 we can see that the lateral tire force estimator is very sensitive to the vehicle parameters; however, the parameter estimation enhances the robustness. Note that the results of case (i) and (iii) are almost identical.

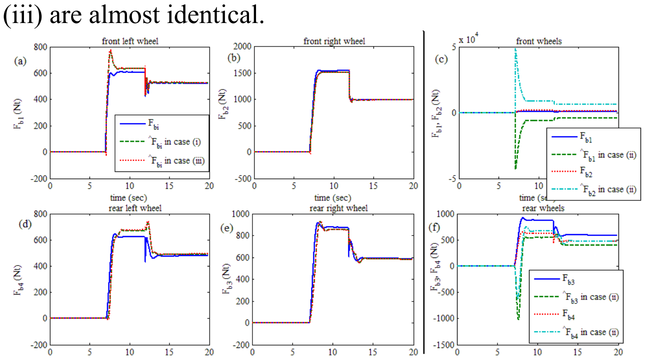

Figure 8: Real and estimated lateral tire forces. The results of case (i) and (iii) are shown in (a)(b)(d)(e) while the results of case (ii) are shown in (c)(f).

Figure 9 shows the results of parameter estimation. The estimated mass converges to the true value immediately after the parameter estimator turns on at t=5sec. However the estimated moment of inertia and the displacement of C.G. do not converge to the true values. Although the estimation of I_z and s is poor, the inaccurate I_z and s have little effects on the lateral tire force estimation. Therefore we conclude that the lateral tire force estimator is sensitive to m, but not to I_z and s. Hence the tire force estimation is satisfactory as long as the vehicle mass is restored to the correct value.

IV. CONCLUSION

In this paper, we proposed a robust tire force estimation algorithm which is able to identify the longitudinal and lateral tire forces of *each* wheel and is robust w.r.t. variations in vehicle parameters. The dependency between the longitudinal and lateral tire forces were taken into account explicitly by introducing the friction ellipse into the tire force estimator. In addition, we proposed to estimate the vehicle's parameters on- line to alleviate the influence of parameter variations on the lateral tire force estimation. Simulations were conducted to verify the proposed algorithm. The results showed that the estimation is satisfactory, even under parameter variations and sudden changes of road conditions.

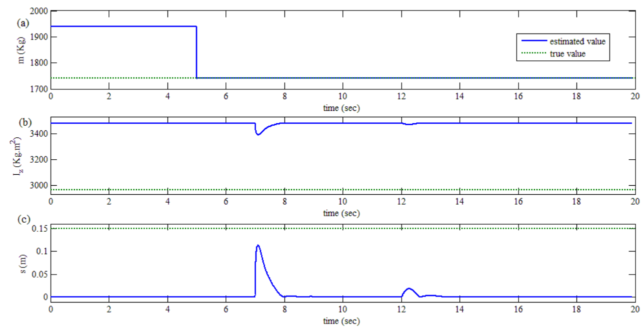

Figure 9: Estimated parameters (a) mass (b) moment of inertia, and (c) displacement of the vehicle's C.G. Solid line: estimated value. Dotted line: true value.

REFERENCES

[1] L. Li, F.-Y. Wang, and Q. Zhou, "Integrated Longitudinal and Lateral Tire/Road Friction Modeling and Monitoring for Vehicle Motion Control," *IEEE Transactions on Intelligent Transportation Systems,* vol. 7, pp. 1-19, 2006.

[2] F. Gustaffson, "Slip-Based Tire-Road Friction Estimation," *Automatica,* vol. 33, pp. 1087-1099, 1997.

[3] J. Wang, L. Alexander, and R. Rajamani, "Friction Estimation on Highway Vehicles Using Longitudinal Measurements," *ASME Transactions on Journal of Dynamic Systems, Measurement, and Control,* vol. 126, pp. 265-275, 2004.

[4] J. Yi, L. Alvarez, and R. Horowitz, "Adaptive Emergency Braking Control with Underestimation of Friction Coefficient," *IEEE Transactions on Control Systems Technology,* vol. 10, pp. 381-392, 2002.

[5] L. Alvarez, J. Yi, and R. Horowitz, "Dynamic Friction Model-Based Tire-Road Friction Estimation and Emergency Braking Control," *ASME Transactions on Journal of Dynamic Systems, Measurement, and Control,* vol. 127, pp. 22-32, 2005.

[6] J.-O. Hahn, R. Rajamani, and L. Alexander, "GPS-Based Real-Time Identification of Tire-Road Friction Coefficient," *IEEE Transactions on Control Systems Technology,* vol. 10, pp. 331-343, 2002.

[7] L. R. Ray, "Nonlinear Tire Force Estimation and Road Friction Identification: Simulation and Experiments," *Automatica,* vol. 33, pp. 1819-1833, 1997.

[8] W. Cho, J. Yoon, S. Yim, B. Koo, and K. Yi, "Estimation of Tire Forces for Application to Vehicle Stability Control," *IEEE Transactions on Vehicular Technology,* vol. 59, pp. 638-649, 2010.

[9] G. Baffet, A. Charara, and D. Lechner, "Estimation of Vehicle Sideslip, Tire Force and Wheel Cornering Stiffness," *Control Engineering Practice,* vol. 17, pp. 1255-1264, 2009.

[10] H. B. Pacejka and E. Bakker, "The Magic Formula Tyre Model," *Vehicle System Dynamics,* vol. 21, pp. 1-18, 1993.

[11] J. Y. Wong, *Theory of Ground Vehicles*, 3 ed.: John Wiley & Sons, Inc. , 2001.

[12] G. Genta, *Motor Vehicle Dynamics : Modeling and Simulation*: World Scientific, 1997.

[13] P. S. Hingwe, *Robustness and Performance Issues in the Lateral Control of Vehicles in Automated Highway Systems*: Ph.D. Dissertation, University of California, Berkeley, 1997.